Copper (II) Halide Complexes of aminopyridines: Synthesis, Structure, and Magnetic Behavior of neutral compounds of 5-IAP: (5-IAP)₂CuCl₂•H₂O, [(5-IAP)₂CuBr₂]₂, (5-IAP)₂CuBr₂ and (5-IAP)₃CuCl₂•nH₂O (5IAP = 2-amino-5-iodopyridine)

Nathan V. Huynh,^a Lixin Li,^{a+} Christopher P. Landee,^b Louise N. Dawe,^c Diane A. Dickie,^d Mark M. Turnbull^a and Jan L. Wikaira^e

^a Carlson School of Chemistry and Biochemistry, Clark University, Worcester, MA 01610 USA; ^b Department of Physics, Clark University, Worcester MA 01610 USA; ^cDepartment of Chemistry and Biochemistry, Wilfrid Laurier University, Waterloo, ON Canada; ^dDepartment of Chemistry, University of Virginia, Charlottesville, VA, 22904 USA ^c School of Physical and Chemical Sciences | Te Kura Matū, University of Canterbury | Te Whare Wānanga o Waitaha, Private Bag 4800, Christchurch, New Zealand

ABSTRACT

Reaction of 2-amino-5-iodopyridine (5IAP) with copper(II) bromide or chloride in alcoholic solution led to four coordination complexes: $[(5\text{-IAP})_2\text{CuCl}_2](\text{H}_2\text{O})$ (1), $(5\text{-IAP})_2\text{CuBr}_2$ (2), $[(5\text{-IAP})_2\text{CuBr}_2]_2$ (3) and $[(5\text{-IAP})_3\text{CuCl}_2](\text{H}_2\text{O})_n$ (4). The compounds were characterized by single crystal X-ray diffraction and variable temperature magnetic susceptibility measurements. 1 crystallizes as monomeric units with the 5IAP ligands in the *syn*-conformation and one lattice water molecule. 2 also exhibits *syn*-conformation 5IAP ligands, but forms a common bromide bibridged dimer structure. 3 is a conformational polymorph of 2 with *anti*-oriented 5IAP ligands. Long Cu···Br contacts link the molecules into chains. 4 crystallizes with 1.67 lattice water molecules, disordered over three positions. All four compounds exhibit strong halogen bonding. Variable field and temperature magnetic data were obtained on 1-3. 1 is paramagnetic, with no indication of magnetic exchange down to 1.8 K. 2 is well modeled as an antiferromagnetic dimer (J/k_B = -22 K) with significant antiferromagnetic interactions between the dimers. 3 is well modeled as a uniform antiferromagnetic chain (J/k_B = -6 K) with weak interchain interactions.

Keywords: Copper (II); magnetism; X-ray structures; aminopyridines

⁺ Present address: Third Harmonic Bio, 130 Prospect St, Cambridge, MA 02139.

INTRODUCTION

Molecular magnetism is a field of research that employs a knowledge of structure, bonding, and geometry to gain an understanding of fundamental magnetic properties at the molecular level. The field is multidisciplinary and involves both synthetic and theoretical chemistry to design and synthesize materials that have targeted magnetostructural correlations.¹ A variety of variables can be controlled including the source of magnetic moment² and the choice of ligand(s) because their steric and electronic properties will affect the coordination geometry of a complex and the potential magnetic superexchange pathways.^{3, 4, 5} Families of coordination complexes are important in their potential applications in microbiological systems,⁶ pharmaceuticals,⁷ spintronics, and quantum computing,⁸ as well as magnetism.

One aspect of magnetic exchange which has been of interest, is understanding two potential magnetic superexchange pathways, the bihalide and the two-halide superexchange pathways. A key difference between the pathways is that in the bihalide pathway, exchange occurs through the bridging halide ions, while in the two-halide pathway, exchange occurs via interactions between the halide ions. The pathways are shown in Scheme 1, where M is a paramagnetic metal ion and X is a halide ion. In the bihalide pathway, magnetic exchange occurs as a result of the nature of the ligand-metal bonds and how the antibonding orbitals relate between the metal centers. Omparatively, in the two-halide pathway, magnetic exchange occurs due to spin delocalization from the transition metal ion to the halide ions and the manner in which the overlap of orbitals on the halide ions allows for magnetic interactions. The lattice structure of the compound will determine the type of pathway a metal halide complex may exhibit in the solid state.



Scheme 1. a) The bihalide magnetic exchange pathway. b) The two-halide magnetic exchange pathway

Many research groups have been studying the effects of changing the metal ion in families of metal halide coordination compounds, including cobalt, ¹³ iron, ¹⁴ and chromium. ¹⁵ One of our research interests has been investigating copper (II) complexes of such systems. We are interested in complexes of copper (II) due to its single unpaired electron, a quantum lower

limit. In addition, although qualitative relationships have been established regarding both the bihalide and two-halide superexchange pathways, to date there are insufficient data to enable formulation of a quantitative relationship between structural parameters and magnetic properties. For such studies, the formulae of the desired products are L₂CuX₂ and (LH)₂CuX₄, for neutral complexes and salts, respectively, where L is an organic-based ligand in the neutral compounds and LH is the protonated cation in the salts. In some prior studies, 2-amino-5-halo-substituted pyridine compounds have been used as L where X was either chloride or bromide. We have reported data on tetrahalidocuprate salts of 2-amino-5-fluoropyridine (5-FAP), ¹⁶ 2-amino-5-chloropyridine (5-CAP), 2-amino-5-bromopyridine (5-BAP), ^{17, 18, 19} and 2-amino-5-iodopyridine (5-IAP). ^{20, 21, 22} Recently, we have studied and reported data on the corresponding neutral complexes using the 5-CAP and 5-BAP ligands. ²³ In an effort to expand such studies in the hopes of developing quantitative magnetostructural correlations, presented here are the syntheses, structures, and magnetic behavior of some neutral compounds of 5-IAP: [(5-IAP)₂CuCl₂](H₂O) (1), (5-IAP)₂CuBr₂(2), [(5-IAP)₂CuBr₂]₂ (3) and [(5-IAP)₃CuCl₂](H₂O)_n (4).

EXPERIMENTAL

2-Amino-5-iodopyridine (5-IAP) was purchased from Matrix Scientific and Tokyo Chemical Industry. Copper(II) bromide was purchased from Aldrich Chemical Corp. Copper(II) chloride dihydrate was purchased from J.T. Baker Chemical Co. IR spectra were recorded on a Perkin Elmer Spectrum100FT-IR Spectrometer with an ATR attachment. Powder X-Ray diffraction (XRD) data were recorded on a Bruker AXS D8 Focus powder diffractometer. Combustion analyses were carried out by the Marine Science Institute, University of California, Santa Barbara, CA 93106.

Synthesis

Bis(2-amino-5-iodopyridine)dichloridocopper(II) monohydrate (1)

A solution copper(II) chloride dihydrate (0.170 g, 1.00 mmol) dissolved in 50 mL of methanol was added to a solution of 5IAP (0.440 g, 2.00 mmol) dissolved in 50 mL of methanol. The beaker was partially covered and placed in a cold room at 5°C for slow evaporation. After one month, acicular clusters of yellow-green rods were harvested by filtration, washed with tertbutanol and allowed to air-dry to give 0.139 g (23%). IR (ATR): 3499w, 3417w, 3332m,

3210vw, 1629s, 1593m, 1555m, 1484s, 1386m, 1315w, 1256w, 1150m, 1034m, 825vs, 669w cm⁻¹. CHN calculated (experimental): C 20.27 (20.51), H 2.04 (1.95), N 9.46 (9.73).

Bis(2-amino-5-iodopyridine)dibromidocopper(II) (2)

A solution of CuBr₂ (0.226g, 1.01 mmol) dissolved in 50mL of ethanol was added to a solution of 2-amino-5-iodopyridine (0.444g, 2.02 mmol) that was dissolved in 50mL of ethanol. The resulting solution was then left at room temperature to evaporate slowly. After ~3 days, black crystals were harvested by vacuum filtration and allowed to dry, giving a yield of 0.372g (56.1%). IR (ATR): 3436m, 3335m, 3202w, 1623s, 1590w, 1549s, 1486s, 1393m, 1331w, 1316w, 1255m, 1149m, 1052w, 1035w, 893m, 822s, 730m, 667w, 626w cm⁻¹. CHN calculated (experimental): C 18.11 (18.28), H 1.52 (1.67), N 8.45 (8.75).

Bis[bis(2-amino-5-iodopyridine)dibromidocopper(II)] (3)

A solution of CuBr₂ (0.223g, 1.00 mmol) dissolved in 40mL of methanol was added to a solution of 2-amino-5-iodopyridine (0.440g, 2.00 mmol) dissolved in 40mL of methanol. The resulting solution was then covered with lightly perforated parafilm and left at room temperature to evaporate slowly. After ~10 days, dark, forest green, prismatic crystals were harvested by vacuum filtration and allowed to dry, giving a yield of 0.361g (54.4%). IR (ATR): 3444w, 3409w, 3338w, 3286w, 3062w, 1621s, 1608s, 1551m, 1479s, 1379m, 1314m, 1251w, 1144m, 1086w, 1028m, 973w, 912m, 821s, 733w, 666m cm⁻¹. CHN calculated (experimental): C 18.11 (18.19), H 1.52 (1.91), N 8.45 (8.16).

Tris(2-amino-5-iodopyridine)dichloridocopper(II) n-hydrate (4)

Compound 4 was isolated in small amounts as a by-product of the synthesis of 1. The flat plates were readily distinguished from the rods of 1. Both were yellow/brown depending upon thickness and thus color was not a reliable indicator. Only sufficient material for single crystal X-ray diffraction and IR was obtained. IR (ATR): 3413m, 3318m, 3200w-br, 1637s, 1617s, 1594m, 1482s, 1388s, 1318m, 1251m, 1153m, 1088m, 1020m, 923w, 907w, 824s, 741w cm⁻¹.

Magnetic data collection

Magnetic susceptibility data were collected using a Quantum Design MPMS-XL SQUID magnetometer. Samples were finely ground and were packed into gelatin capsules. The magnetization was measured using magnetic fields from 0 to 50 kOe at 1.8 K. As the field returned to 0 kOe, several data points were collected to check for hysteresis effects; none were observed. Magnetization was then measured from 1.8 to 310 K in a 1 kOe field. Data were corrected for the background signal of the gelatin capsule and sample holder (measured independently), the temperature independent paramagnetism of the copper(II) ion and the diamagnetism of the constituent atoms as estimated from Pascal's constants. The Hamiltonian $H = -J \sum S_1 \cdot S_2$ was used for fitting of magnetic data. Best fit parameters were determined by least-squares minimizations between the model and experimental data. Fitting was performed using Origin software from OriginLab Corporation, Northampton, Massachusetts, USA

X-ray data collection

Data for 1 and 2 were collected on a Bruker Kappa DUO diffractometer. Data collection and reduction were made using Bruker Instrument Services v.2017.5.0 and SAINT v.8.40B. ²⁴ Absorption corrections were performed using SADABS. ²⁵ Data for 3 were obtained using a Bruker/Siemens SMART APEX instrument. Cell parameters were retrieved using SMART²⁶ software and refined using SAINTPlus²⁷ on all observed reflections. Absorption corrections were performed using SADABS. ²⁵ Data for 4 were collected on a Rigaku Saturn CCD area detector and were collected and processed using CrystalClear; ²⁸ a numerical absorption correction was applied. ²⁹ The crystal structures were solved using SHELXS-2014 ³⁰ and refined via least squares analysis using SHELXL-2018. ³¹ All non-hydrogen atoms were refined anisotropically. Hydrogen atoms bonded to carbon atoms were added in calculated positions and refined using a riding model with fixed isotropic thermal parameters. Hydrogen atoms bonded to nitrogen and oxygen atoms were located in the difference map and their positions refined using fixed isotropic thermal parameters. Crystallographic information and data collection details can be found in Table 1. The structures have been deposited with the CCDC as: 1, 2277029; 2, 2277030; 3, 2277031; 4, 2277032.

Table 1: Crystal Refinement Data

	1	2	3	4
Formula	$C_{10}H_{12}Cl_2CuI_2N_4O$	$C_{20}H_{20}Br_{4}Cu_{2}I_{4}N_{8} \\$	$C_{10}H_{10}Br_2CuI_2N_4$	$C_{15}H_{15}Cl_{2}CuI_{3}N_{6}O_{1.67} \\$
Mol. Wt.	592.48	1326.76	663.38	821.15
Temp. (K)	100(2)	100(2)	88(2)	113(2)
λ(Å)	0.71073	0.71073	0.71073	0.7107
Cryst. Sys.	Monoclinic	Triclinic	Triclinic	Monoclinic
Space group	P2/n	P-1	P-1	P2 ₁ /c
(a, Å)	7.6928(8)	8.1896(9)	4.9130(7)	16.948(3)
(b, Å)	6.4891(6)	10.3737(10)	7.9536(11)	8.9428(13)
(c, Å)	16.2056(14)	10.6620(11)	10.2010(13)	16.320(2)
$(\alpha,^{\circ})$	90	90.269(3)	92.407(2)	90
$(\beta,^{\circ})$	96.365(3)	108.941(3)	100.863(2)	92.290(3)
$(\gamma,^{\circ})$	90	108.559(3)	98.438(2)	90
Vol. (Å ³)	803.99(13)	806.29(15)	386.24(9)	2471.6(6)
Z	2	1	1	4
Size (mm ³)	0.13x0.10x0.04	0.08x0.08x0.06	0.21x0.21x0.06	0.62x0.46x0.21
θ range (°)	2.529-28.298	2.034-28.321	2.596-26.379	2.576-27.678
Rfln. Total	11946	20915	5472	33301
Rfln. Ind.[R _{int}]	2011[0.0446]	4013[0.0619]	1508[0.0260]	5757 [0.0222]
Data/restr./para	2011/3/101	4013/0/184	1508/0/94	5757/3/292
GooF on F ²	0.998	0.988	1.165	1.167
Final R1/wR2	0.0213(0.0381)	0.0300/0.0458	0.0234/0.0588	0.0319/0.0653
Final R1/wR2 (all data)	0.0337(0.0406)	0.0503/0.0504	0.0248/0.0593	0.0323/ 0.0655
Final peak/hole (e.Å ⁻³)	0.54/-0.54	0.07/.0.77	0.663/-1.409	1.87/-1.10 (both near
rmai peak/noie (e.A ')	0.34/-0.34	0.97/-0.77	(near I)	I atoms)

RESULTS

Synthesis

Reaction of the appropriate copper(II) halide salt with 2-amino-5-iodopyridine (5-IAP) in alcohol solution gave crystals of **1-4** (Scheme 2). Compounds **2** and **3** are occasionally cocrystallized polymorphs, but could be identified and manually separated based on color and morphology (**2**, dark green, prisms; **3**, black, rods or plates). Although both compounds can be

prepared via a 2:1 stoichiometry, the formation of **2** was favored by a lower ligand:metal ratio and the use of ethanol as solvent, while the formation of **3** was favored by increasing the ratio and using methanol as solvent.

Scheme 2. Synthesis of compounds 1-4.

Structures

Compound 1 crystallizes in the monoclinic space group *P2/n*. The asymmetric unit comprises one 5IAP ligand, one chloride ion and one-half Cu(II) ion (located on a two-fold rotation axis), and one-half of a lattice water molecule (also located on a two-fold axis, see Figure 1). Selected bond lengths and angles are provided in Table 2. The Cu-N and Cu-Cl bond lengths are comparable to those observed in (5-bromo-2-aminopyridinium)₂CuCl₂.³² We find no prior reports of structures of transition metal complexes of 5IAP itself for comparison.³³ The Cu-coordination sphere shows a distinct flattening from tetrahedral due to the Jahn-Teller distortion and steric bulk of the 5IAP ligand, with a mean trans angle of 149.4°.³⁴

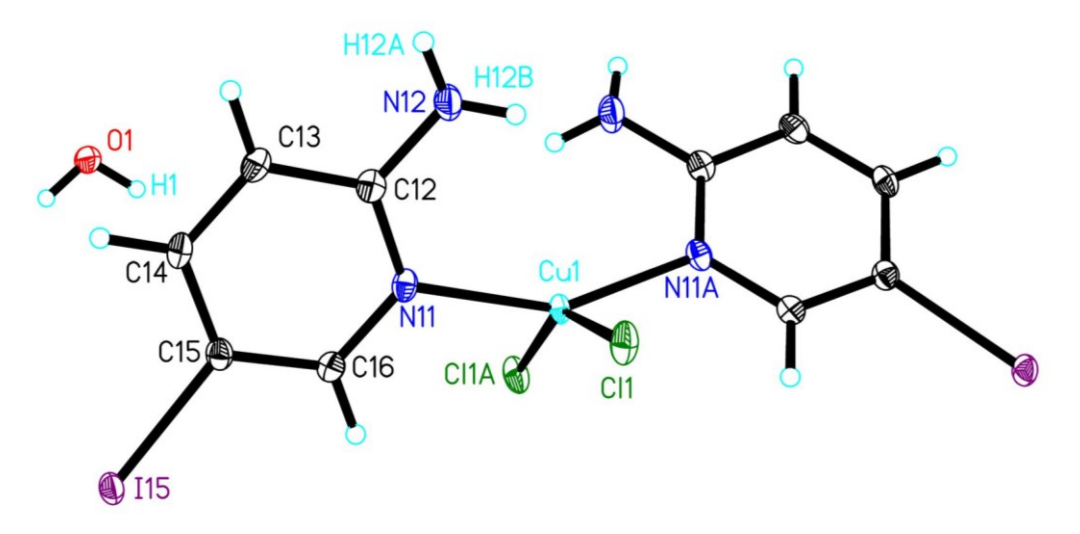


Figure 1. The molecular unit of **1** showing 50% probability ellipsoids. Hydrogen atoms are shown as spheres of arbitrary size. Only the asymmetric unit, Cu-coordination sphere and those hydrogen atoms whose positions were refined are labeled.

The 5IAP rings are virtually planar (mean deviation of constituent atoms = 0.0076 Å); the ligands are inclined 47.7° to each other in a *syn*-conformation.³⁵ Although the *syn*-conformation generally leads to halide bi-bridged dimer formation,³⁵ such is not observed in 1. Bond lengths and angles within the 5IAP ring are comparable to those observed in the salts (5IAPH)₂CuCl₄³⁶ and (5IAPH)₈ [Mn₄Cl₁₀(H₂O)₈] Cl₆.³⁷ Hydrogen and halogen bonding are both exhibited in the structure of 1 (see Figure 2). Water molecules serve as hydrogen bond donors to chloride ions (see Table 3) and the amino-groups serve as hydrogen bond donors to the water molecules. Strong, Type II halogen bonds are observed between the chloride ions and iodine atoms on the 5IAP ligands (Figure 2 and Table 4) with a Cl···I distance of 3.46(1) Å. The intermolecular interactions result in an overall layer structure for 1 (see Figure 3) with the layers parallel to the *ac*-plane with the water molecules interspersed between the layers. The layers are interconnected by both the hydrogen and halogen bonds.

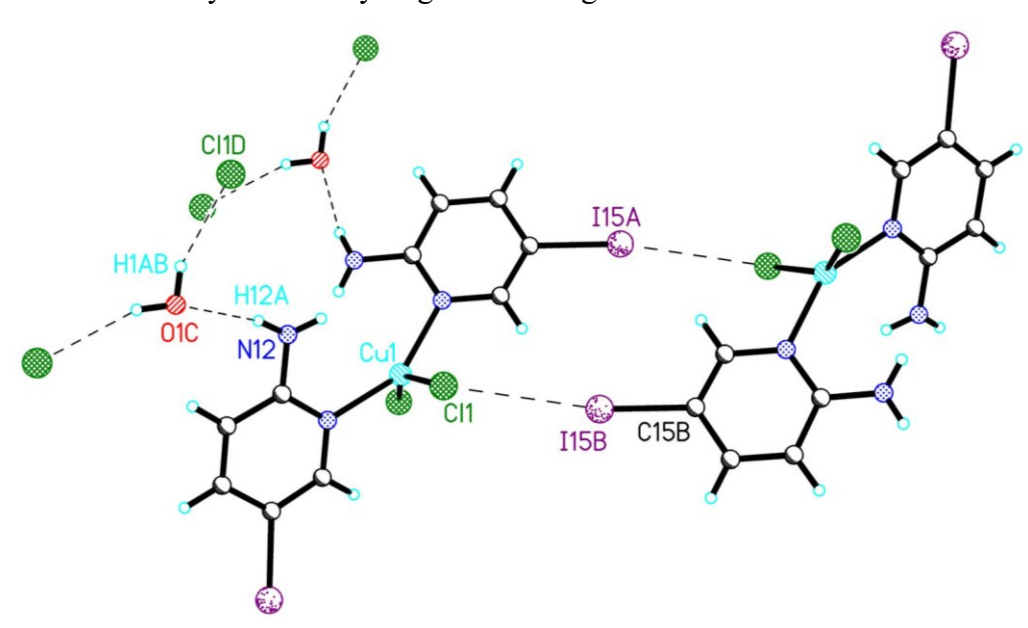


Figure 2. Hydrogen and halogen bonding in 1. Sym. Ops. I15a -x+0.5, y, -z+0.5; I15b = 1-x, 1-y, z-0.5; O1C = 1-x, 3-y,1-x; Cl1D = x, y+1, z.

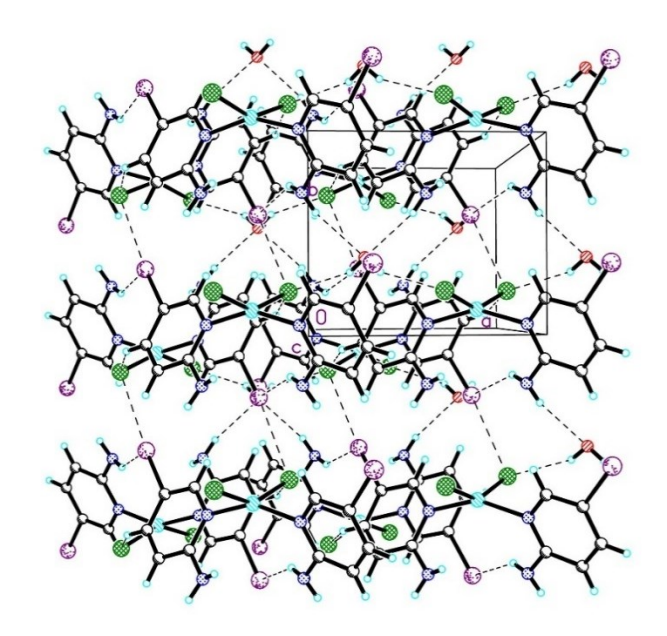


Figure 3. The packing of 1 viewed parallel to the c-axis. Dashed lines represent halogen and hydrogen bonds.

Table 2: Bond Lengths (Å) and angles (°) in 1-4.

	1	2	3	4
Cu1-N11	1.992(2)	1.996(3)	1.986(4)	2.213(3)
Cu1-N21		1.999(3)		2.015(3)
Cu1-N31				2.018(3)
Cu1-X1	2.2448(7)	2.5013(7)	2.4261(5)	2.3437(11)
Cu1-X2		2.4351(7)		2.3992(11)
Cu1-X1 ^B		2.8120(7)		
Cu1-Cl2				
X1-Cu1-X1 ^A /N21	147.22(5)	87.65(2)	180	86.98(10)
X1-Cu1-X2		175.07(3)		145.43(4)
X2-Cu1-X1 ^B /N31		97.01(2)		90.01(10)
N11-Cu1-N11 ^A /N21	151.58(14)	164.33(14)	180	
N11-Cu1-X1	93.73(7)	88.05(10)	89.88(11)	105.10(10)
N11-Cu1-X2		89.63(10)		109.46(10)
N21-Cu1-N31				168.86(13)

Symm. Op.: $^{A} = \frac{1}{2}$ -x, y, $\frac{1}{2}$ -z; $^{B} =$ -x, 2-y, 2-z;

Table 3
Hydrogen bonding for 1-4.

			$d(D\cdots A)$ Å	∠(DHA)°	Sym.Op.
N12-H12A···O1 ^A	0.828(17)	2.26(2)	3.072(3)	166(3)	-x, 3-y, z-1/2
O1-H1···Cl1 ^B	0.815(17)	2.40(2)	3.1536(13)	155(3)	1-x, 2-y, 1-z
N12-H12A···Br1	0.83(5)	2.99(5)	3.394(6)	112(4)	x-1, y, z
N12-H12A···Br1 ^B	0.80(6)	2.68(6)	3.408(4)	152(5)	-1-x, -y, -1-z
N12-H12A···Cl2	0.825(19)	2.46(3)	3.254(4)	162(5)	
N22-H22A···Cl2	0.91(5)	2.51(5)	3.293(4)	145(4)	
N32-H32A···Cl1	0.87(6)	2.55(5)	3.278(4)	158(5)	
	O1-H1···Cl1 ^B N12-H12A···Br1 N12-H12A···Br1 ^B N12-H12A···Cl2 N22-H22A···Cl2	O1-H1···Cl1 ^B 0.815(17) N12-H12A···Br1 0.83(5) N12-H12A···Br1 ^B 0.80(6) N12-H12A···Cl2 0.825(19) N22-H22A···Cl2 0.91(5)	O1-H1···Cl1B 0.815(17) 2.40(2) N12-H12A···Br1 0.83(5) 2.99(5) N12-H12A···Br1B 0.80(6) 2.68(6) N12-H12A···Cl2 0.825(19) 2.46(3) N22-H22A···Cl2 0.91(5) 2.51(5)	O1-H1···Cl1B 0.815(17) 2.40(2) 3.1536(13) N12-H12A···Br1 0.83(5) 2.99(5) 3.394(6) N12-H12A···Br1B 0.80(6) 2.68(6) 3.408(4) N12-H12A···Cl2 0.825(19) 2.46(3) 3.254(4) N22-H22A···Cl2 0.91(5) 2.51(5) 3.293(4)	O1-H1···Cl1B 0.815(17) 2.40(2) 3.1536(13) 155(3) N12-H12A···Br1 0.83(5) 2.99(5) 3.394(6) 112(4) N12-H12A···Br1B 0.80(6) 2.68(6) 3.408(4) 152(5) N12-H12A···Cl2 0.825(19) 2.46(3) 3.254(4) 162(5) N22-H22A···Cl2 0.91(5) 2.51(5) 3.293(4) 145(4)

Table 4
Halogen bonding for 1-4.

Cmpd		$d_{X\cdots X}(A)$	∠Cu/C-X···X'(°)	∠xx'-c (°)
1	Cu-Cl1···I15B-C15B ^A	3.46(1)	117.5(2)	169.8
2	Cu1-Br2···I1 ^B -C15 ^B	3.52(1)	107.2(6)	174.0(5)
	Cu1-Br2···I2 ^C -C25 ^C	3.56(1)	107.2(6)	176.9(5)
	$C15^{B}$ - $I1^{B}$ ··· $I2^{C}$ - $C25^{C}$	4.11(1)	125.5(5)	125.3(5)
3	Cu1-Br1···I1 ^D -C15 ^D	3.95(1)	117.3(4)	155.5(5)
	C15-I1···I1 ^D -C15 ^D	4.247	94.2(4)	94.2(4)
4	Cu1-Cl1···I1 ^A	3.35(1)	138.7(5)	178.8(6)
	Cu1-Cl1···I3 ^B	3.40(1)	137.3(5)	172.2(6)
	C15-I1····I2 ^c -C25 ^c	3.84(1)	75.8(4)	160.7(6)
		·	·	·

Compound **2** crystalizes in the triclinic space group P-1. The asymmetric unit comprises two 5IAP ligands, two bromide ions and one Cu(II) ion. The 5IAP ligands lie in the *syn*-conformation and as is typical of such,³⁵ the compound forms a dimeric structure with a bi-halide bridge (Figure 4). The resulting 5-coordinate Cu(II) ions are moderately distorted square pyramidal in geometry (Addison parameter = 0.18).³⁸ The Cu-N and Cu-Br bond lengths are comparable to those observed in the corresponding dimeric compound [(5-methyl-2-aminopyridine)₂Cu Br₂]₂.³⁹ The 5IAP rings are virtually planar [mean deviation of constituent

atoms = 0.0193 Å(N11 ring), 0.0027 Å (N21 ring)] and are nearly co-planar with each other; the angle between the respective planes is only 4.3° . Bond lengths and angles within the 5IAP ring are again comparable to those observed in the salts indicated previously. 36,37

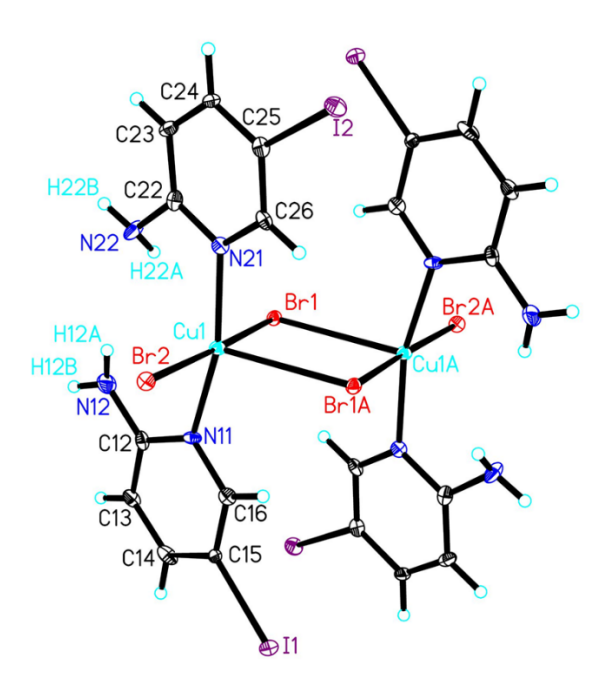


Figure 4. The molecular unit of **2** showing 50% probability ellipsoids. Hydrogen atoms are shown as spheres of arbitrary size. Only the asymmetric unit, Cu-coordination sphere and those hydrogen atoms whose positions were refined are labeled.

Only weak hydrogen bonds are observed in the lattice, likely as a result of the bulky iodine atoms, but strong Type II halogen bonds (d < 3.6Å) are observed between iodine atoms and bromide ions (Figure 5a and Table 4) and a weaker Type I halogen bond (d = 4.11 Å) is observed between iodine atoms. The latter may simply be the result of proximity between 5IAP rings caused by the strong Br···I halogen bonds. The result is that the dimers are stacked parallel to the *a*-axis and adjacent stacks are staggered parallel to the *bc*-face diagonal (Figure 5b).

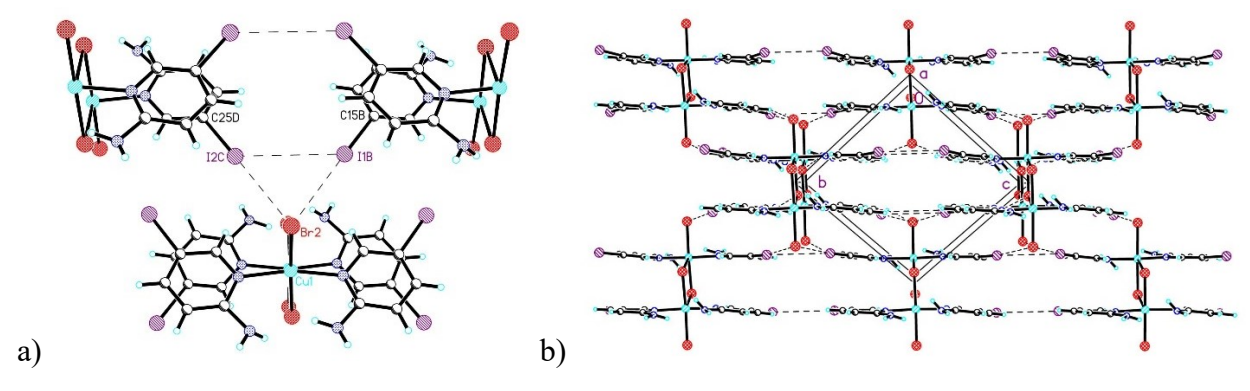


Figure 5. a) Halogen bonding in **2**. Sym. Ops.: I1B -x, 3-y, 2-z; I2C -x 2-y 3-z. b) The packing of **2** viewed parallel to the *a*-axis. All dashed lines represent halogen bonds.

 π -Stacking is observed in the system with the distance between rings = 3.20 Å, the distance between the ring centroids = 3.73 Å and a slip angle of 28.5°.

Compound **3** is a conformational isomer of **2**, but still crystallizes in the triclinic P-1 space group with one 5IAP ligand, one bromide ion and one-half Cu(II) ion, located on an inversion center, comprising the asymmetric unit (Figure 6). The Cu(II) ion lies on a crystallographic inversion center and as such a nearly square planar geometry results (\angle _{Br1-Cu1-N11} = 89.88(11)°). All trans bond angles are 180° as required by symmetry. The Cu(II) bond lengths are comparable to those observed in (5-bromo-2-aminopyridine)₂CuBr₂.³² The 5IAP ligands are again highly planar (mean deviation of constituent atoms = 0.0254Å) and are co-planar as required by symmetry. They are canted 80.8° from the Cu1 coordination plane. Bond lengths and angles within the 5IAP molecules are as observed above.^{36,37}

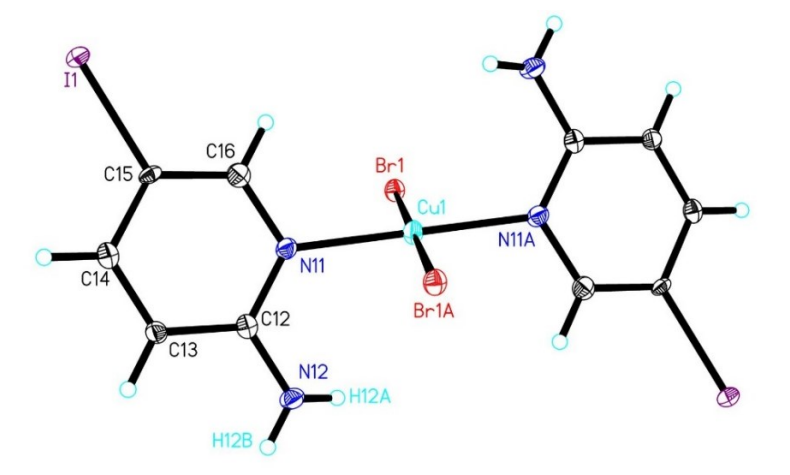


Figure 6. The molecular unit of **3** showing 50% probability ellipsoids. Hydrogen atoms are shown as spheres of arbitrary size. Only the asymmetric unit, Cu-coordination sphere and those hydrogen atoms whose positions were refined are labeled.

The molecules are linked into halide bi-bridged chains parallel to the *a*-axis by long Cu···Br contacts (Figure 7), $d_{Br1···Cu1A} = 4.25 \text{ Å}$, $\angle_{Cu1-Br1···Cu1A} = 90.5^{\circ}$.

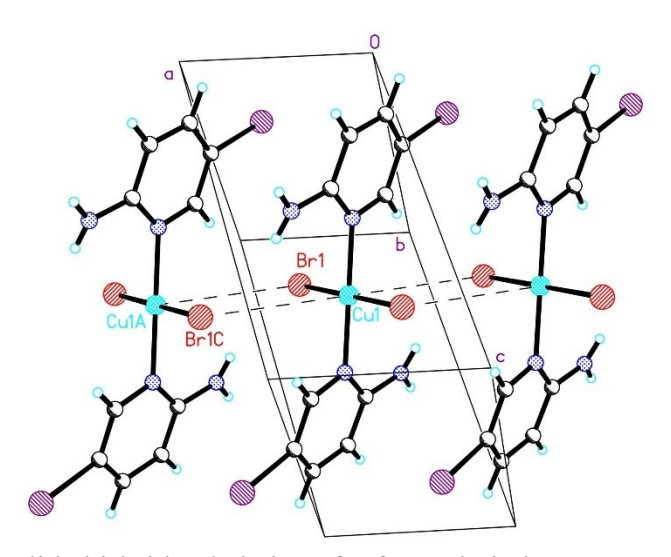


Figure 7. Halide bi-bridged chains of **3** formed via long Cu···Br contacts.

Only weak hydrogen bonding is observed in 3 (Table 3), as was true in 2, but again there are strong, Type II halogen bonds (Table 4) between the iodine atoms and bromide ions, parallel to the *c*-axis (Figure 8a). Weaker, Type I halogen bonds are observed between iodine atoms roughly parallel to the *b*-axis. The bromide bi-bridged chains are linked via those hydrogen and halogen bonds to stabilize the 3D-lattice (see Figure 8b).

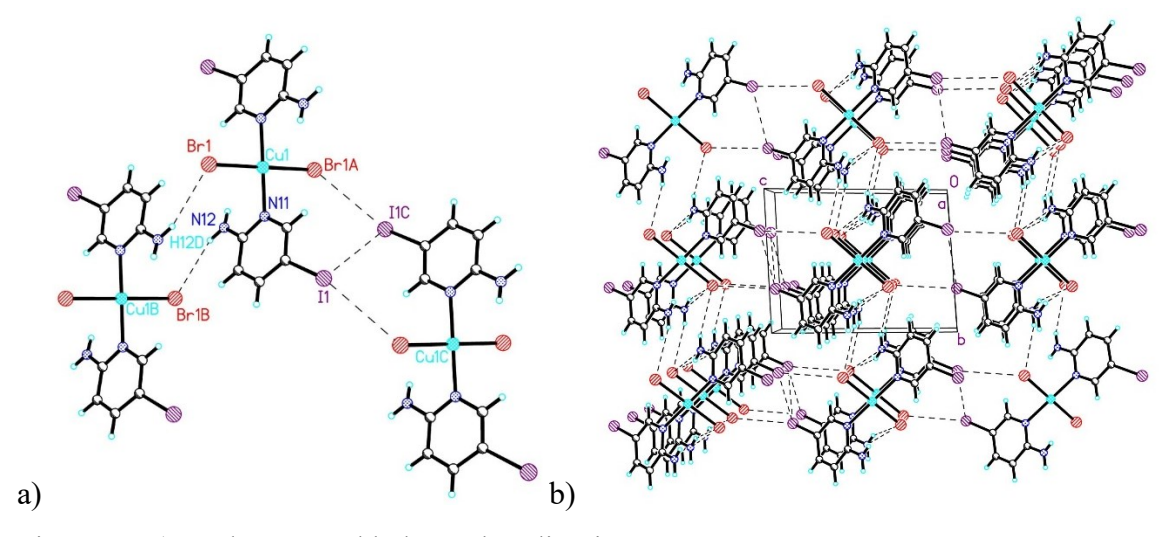


Figure 8. a) Hydrogen and halogen bonding in 3. Sym. Op.: A = -1-x, -1-y, -1-z; B = -1-x, -y, z; C = -x, -1-y, -z. b) The crystal packing of 3 viewed parallel to the a-axis. All dashed lines represent hydrogen and halogen bonds.

On occasion, a small amount of compound 4 co-crystallized with 1 which could be readily identified by color and crystal habit (1, yellow rods; 4, brown plates) and isolated manually from the mixture. 4 crystallizes in the monoclinic space group $P2_1$ /c with a Cu(II) ion, two chloride ions and three 5IAP ligands in the asymmetric unit (Figure 9). In addition, 1.67 water molecules were observed in the lattice, disordered over three positions (O1, O2 and O3 in Figure 9). Attempts to locate and refine the hydrogen atoms on those water molecules failed to improve the refinement. An alternate method, introduction of a solvent mask, removed 16 electrons from the structure, in good agreement with 1.67 water molecules (16.7 electrons). The CIF for the refinement including the solvent mask is available in the supplementary information. The disordered partial water molecules will not be considered further in the discussion.

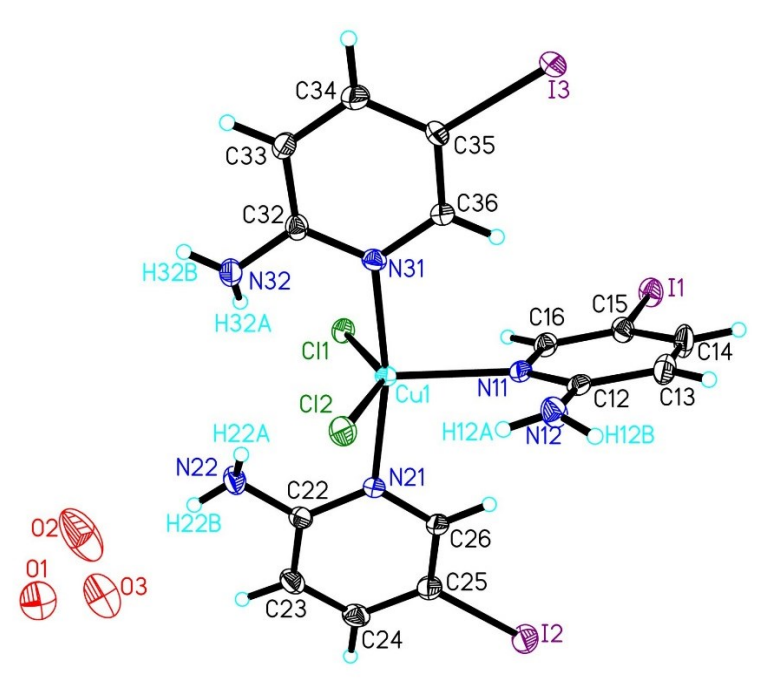


Figure 9: The molecular unit of **4** showing 50% probability ellipsoids. Hydrogen atoms are shown as spheres of arbitrary size. Only the asymmetric unit, Cu-coordination sphere and those hydrogen atoms whose positions were refined are labeled. O1, O2 and O3 represent the disordered sites of 1.67 water molecules.

The geometry about the Cu(II) is significantly distorted square pyramidal with an Addison parameter of 0.39 and N11 lying in the axial coordination site. The equatorial ligands (N21, N31, C11, C12) are roughly planar (mean deviation of constituent atoms = 0.25 Å) with the Cu(II) ion lying 0.45 Å above that plane. As described earlier, the bond lengths and angles within the 5IAP ligands are in good agreement with those previously reported, and they are nearly planer (mean

deviations by ring: N11 = 0.0049 Å; N21 = 0.0124 Å; N31 = 0.0064 Å). The N21 and N31 rings are nearly coplanar (6.4°) and the N11 ring roughly perpendicular to both (74.0° and 78.8° respectively).

Weak intramolecular hydrogen bonds are observed in 4 (Table 3) and strong intermolecular halogen bonds are found linking molecules into a three-dimensional lattice (Table 4, Figure 10). I···Cl distances are 3.3-3.4 Å while I···I distances are 3.8 Å. π -Stacking is also observed between the pseudo-axial 5IAP ligands (see Figure 11) with the distance between the ring centroids = 3.656 Å, a 3.33 Å spacing between the ring planes and a slip angle of 21.4°. The angle between planes of the rings is 6.6°.

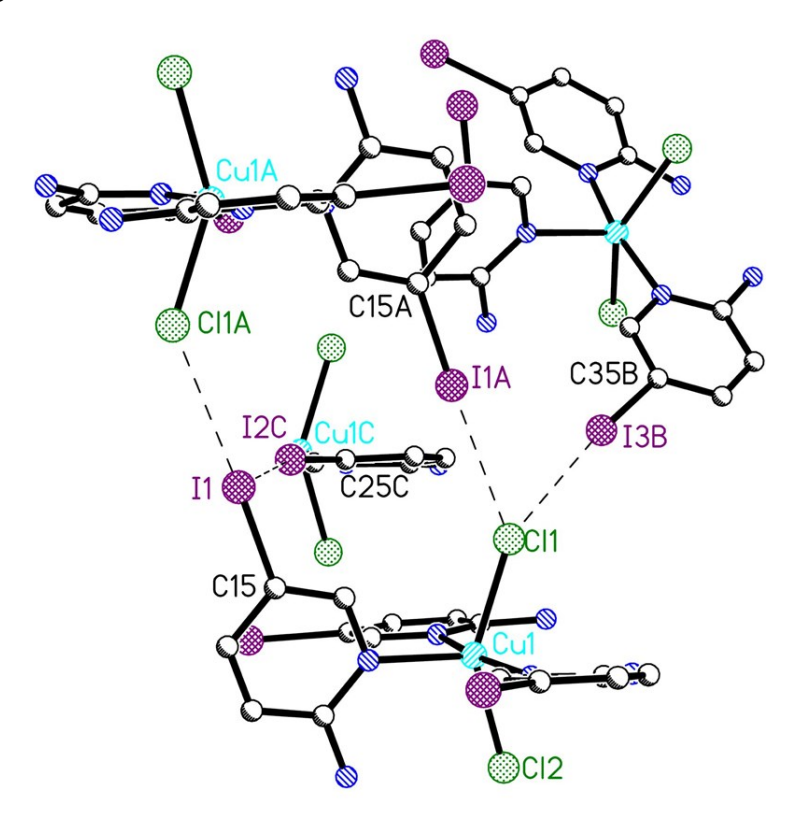


Figure 10. Halogen bonding in **4** (dashed lines). Hydrogen atoms have been removed for clarity. Sym. Ops.: A = 1-x, 1-y, 1-z; B = x, 1.5-y, z-0.5; C = x, y+1 z.

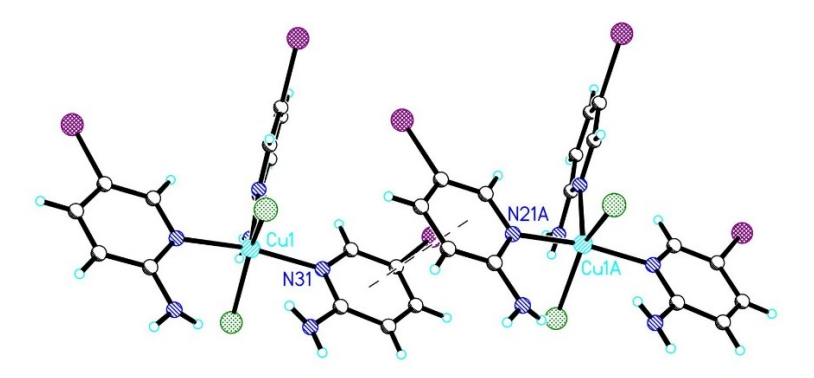


Figure 11. π -Stacking in 4. The dashed line represents the vector between the ring centroids. Sym. Ops.: A = x, y+1, z.

Although there are a number of copper complexes reported with three pyridine rings and two halide ions bonded to the copper ion, virtually all involve terpyridine (as the F, 40 Cl, 41 Br 42 or I^{43} complex) or its derivatives, or a wide variety of other chelating or bridging ligands. We found only one prior report of such a compound where the three pyridine ligands are all monodentate, $(2\text{-amino-}5\text{-trifluoromethylpyridine})_3\text{CuBr}_2$, 44 with a similar, but slightly more distorted square pyramidal geometry (Addison parameter = 0.47). The presence of the amino-substituents in the 2-position of the pyridine rings likely provides a steric blockade in both compounds which prevents coordination of a sixth ligand.

Magnetic Susceptibility Data

The magnetization data for compounds 1, 2, and 3 were collected as a function of applied field between 0-50 kOe. Magnetic susceptibility data were collected as a function of temperature from 1.8-310 K. Insufficient quantities of 4 were obtained to allow measurement of magnetic properties.

M(H) data for 1 at 1.8 K (Figure SI-1) show near saturation of the moment at 50 kOe, reaching 5,870 emu/mol in good agreement with the expected value for a Cu(II) ion with g slightly greater than $2.00.^{1}$ Susceptibility data for 1 rise monotonically with decreasing temperature; no sign of a maximum in χ at low temperature is observed (Figure SI-2). The data were fit to the Curie-Weiss law (Figure 12)⁴⁵ resulting in a Curie constant of 0.443(1) emu-K/mol-Oe and a Weiss constant of zero within the error (Table 5), indicating an absence of magnetic exchange over the temperature range.

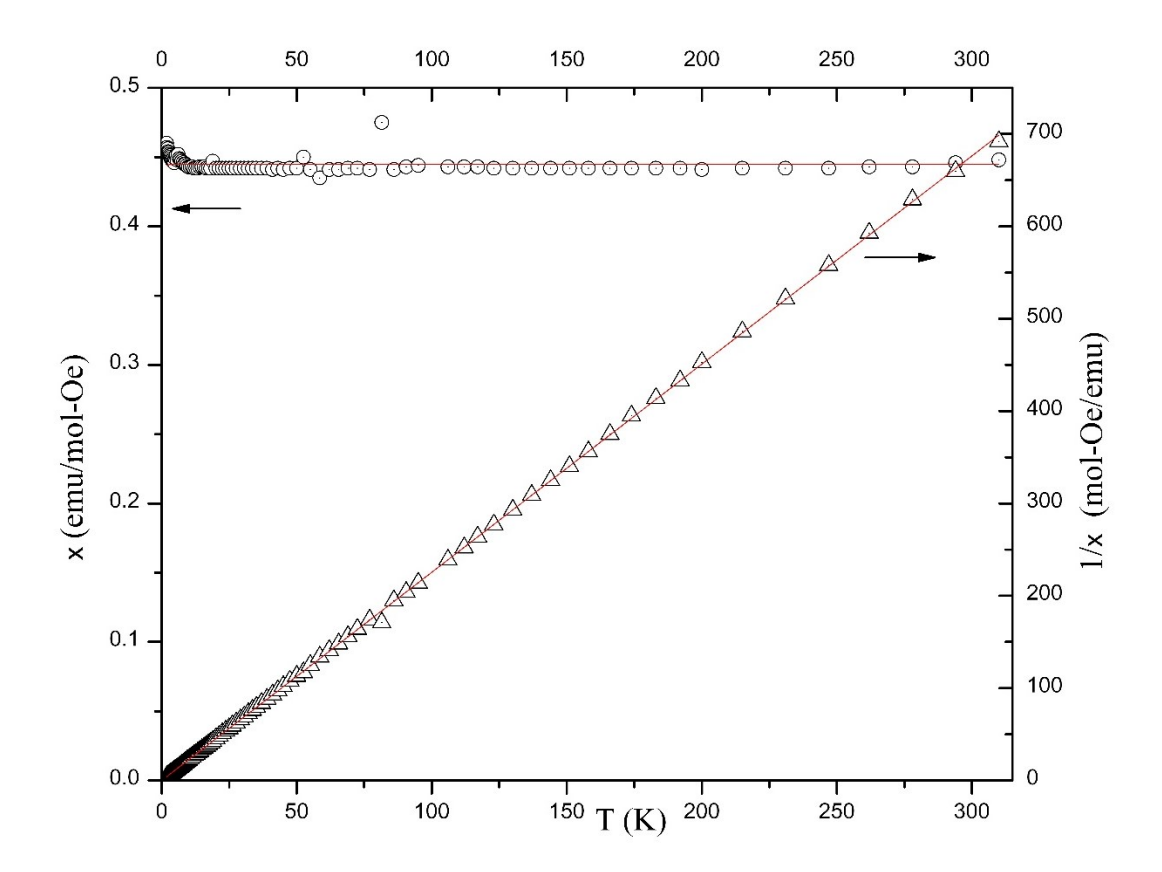


Figure 12. $1/\chi$ (T) data (Δ) and χ T(T) data (\circ) for **1**. The solid lines show the best fit to the Curie-Weiss law.

Table 5. Fitted magnetic parameters for 1-3.

Cmpd	Model	CC (emu- k/mol-Oe	$J/k_{B}\left(K\right)$ $\left\{ cm^{-1}\right\}$	θ (K)	p (%)
1	Curie-Weiss Law	0.443(1)		-0.02(3)	
2	Curie-Weiss Law	0.438(1)		-7.8(3)	
	Dimer χ(T)	0.456(1)	-21.1(1) {-15.1(1)}	-4.4(1)	5.8(1)
	Dimer $\chi T(T)$	0.440(1)	-23.1(3) {-16.5(2)}	-5.3(5)	4.7(3)
3	Curie-Weiss Law	0.400(1)		-4.7(3)	
	Linear chain $\chi(T)$	0.397(3)	-6.1(4) {-4.4(3)}	-0.6(3)	1.6

Linear chain $\chi T(T)$	0.401(1)	-5.9(5)	-0.9(4)	1.0(9)
		{-4.2(3)}		

 $CC = Curie\ Constant;\ \theta = Weiss\ constant;\ p = paramagnetic\ impurity$

M(H) data for **2** at 1.8 K (Figure SI-3) reach 140 emu/mol at 50 kOe, well below the expected value of ~6,000 emu/mol. This suggests a singlet ground state for the bulk material and only a trace paramagnetic impurity is responsible for the observed moment at that temperature. A Curie-Weiss fit to the data above 60 K resulted in a Curie constant of 0.438 emu-K/mol-Oe and Weiss constant of -7.8(3) K, indicating antiferromagnetic interactions (Figure 13).

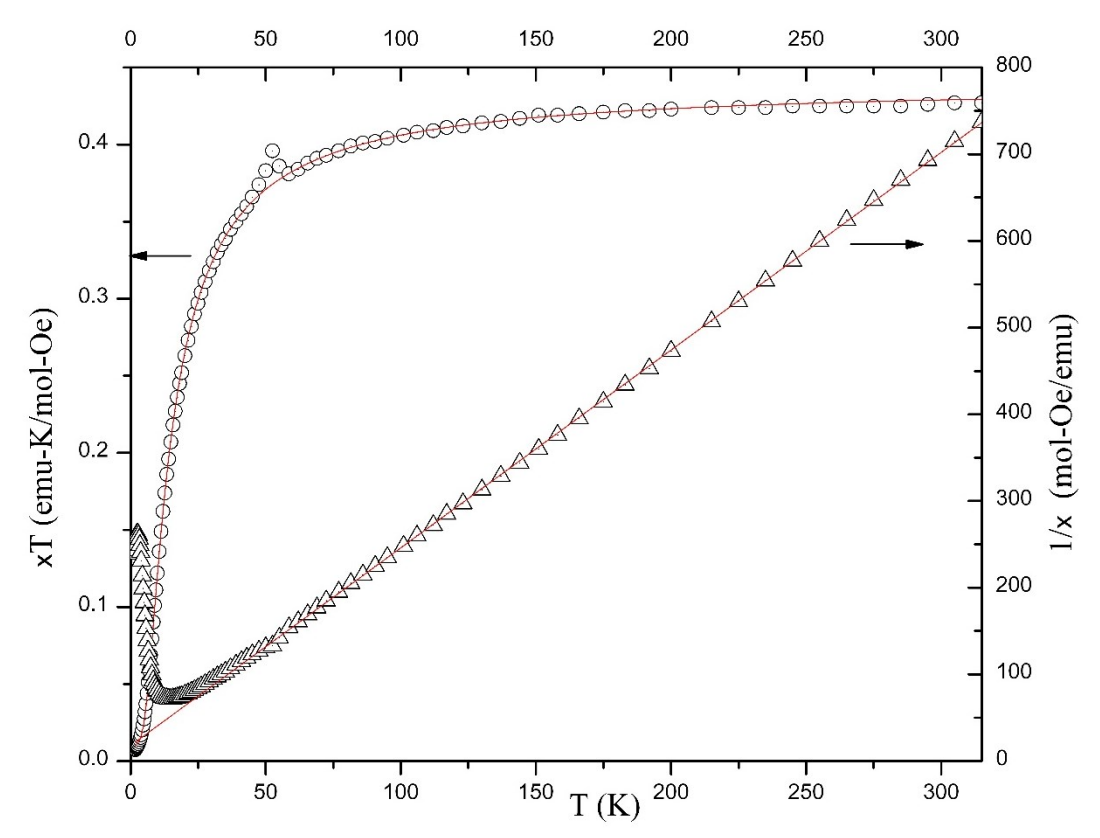


Figure 13. $1/\chi$ (T) data (Δ) and χ T(T) data (\circ) for **2**. The solid lines show the best fit to the dimer model with a Curie-Weiss correction for interdimer interactions. The anomaly at 50 K is trace O_2 .

The temperature dependence of the susceptibility was fitted using the dimer model with a Curie-Weiss correction for interdimer interactions (Figure 14, Table 5).⁴⁵ The abrupt decrease in χ below the maximum confirms the presence of a singlet ground state. The $\chi T(T)$ data were fitted to the same model and good agreement is seen between the fitted parameters (Figure 13, Table 5). As least-squares fits, the fits to the two plots emphasize different regions of the data, with the

 $\chi(T)$ data emphasizing the low temperature region and the $\chi T(T)$ data emphasizing the high temperature region.

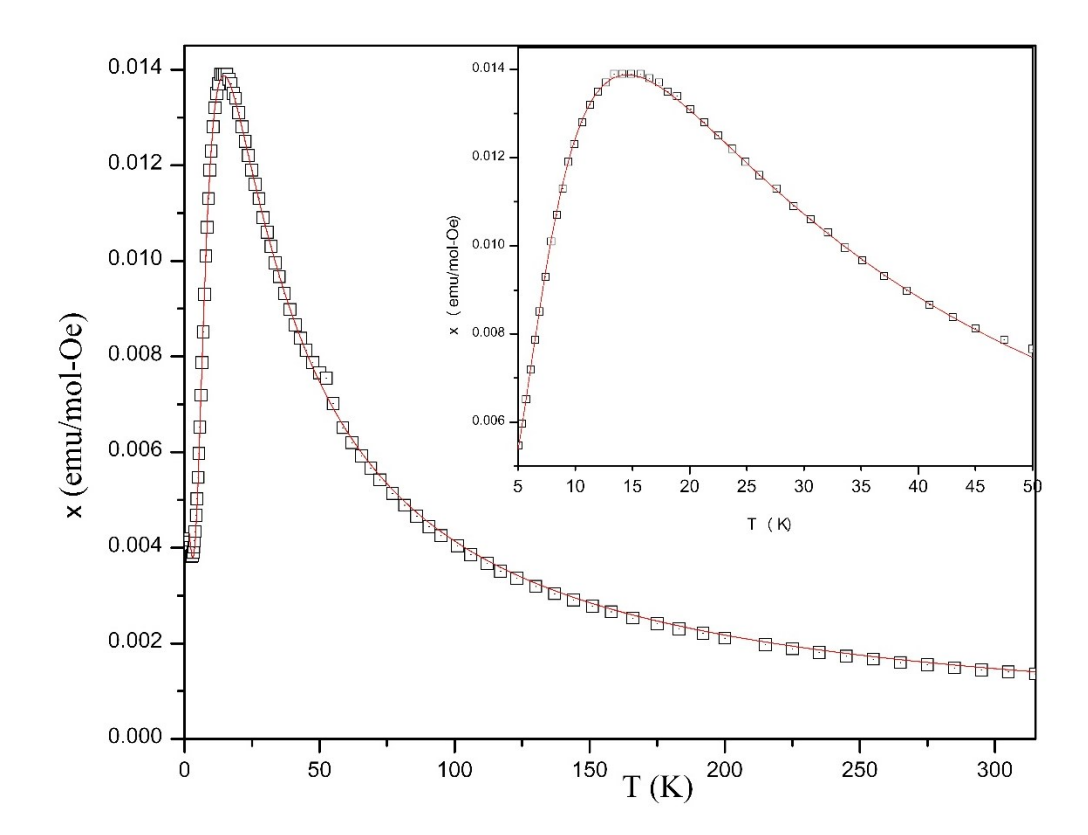


Figure 14. $\chi(T)$ data for 2. The solid lines show the best fit to the dimer model with a Curie-Weiss correction for interdimer interactions. The inset shows an expansion of the region near the maximum in χ . The anomaly near 50 K results from a trace of O_2 .

M(H) data for compound **3** are shown in Figure SI-4. The moment reaches nearly 2000 emu/mol at 50 kOe, about 1/3 of the expected saturation moment, but it is clearly far from saturation. The upward curvature observed is indicative of a low-dimensional antiferromagnet. A Curie-Weiss plot of the data down to 20 K (Figure 15, Table 5) yielded a Curie constant of 0.400(1) emu-K/mol-Oe and θ = -4.7 K, suggesting weaker antiferromagnetic interactions than observed in **2**. The χ (T) data were fit to the uniform chain model with a Curie-Weiss correction for interchain interactions (Figure 16, Table 5) yielding a Curie constant of 0.397 emu/mol-Oe and an antiferromagnetic exchange constant of -6.1(4) K. Results from fitting the χ T(T) plot to the same model are identical within the error (Table 5).

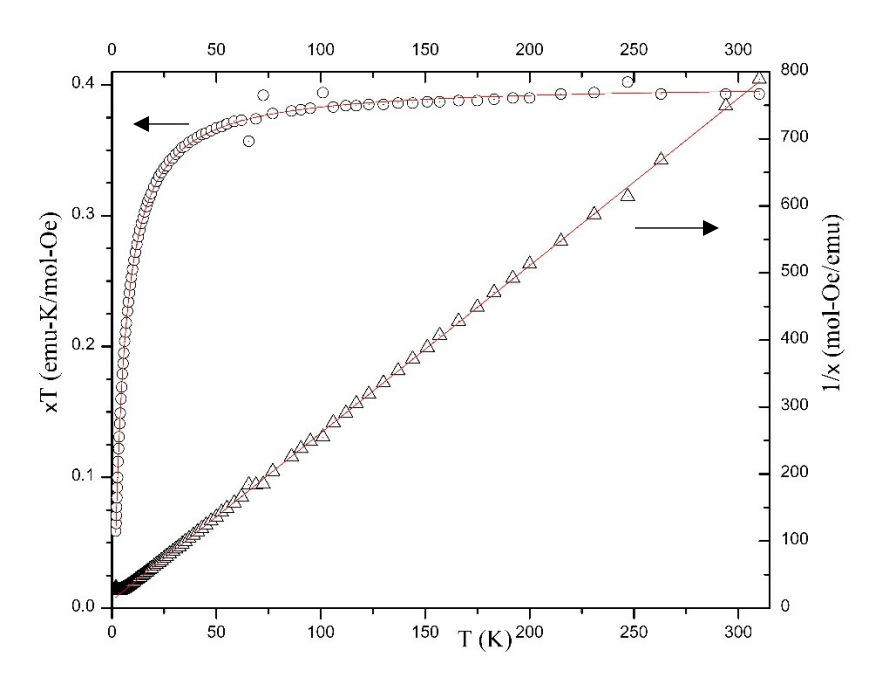


Figure 15. $1/\chi$ (T) data (Δ) and χ T(T) data (\circ) for **3**. The solid lines show the best fit to the linear chain model with a Curie-Weiss correction for interchain interactions.

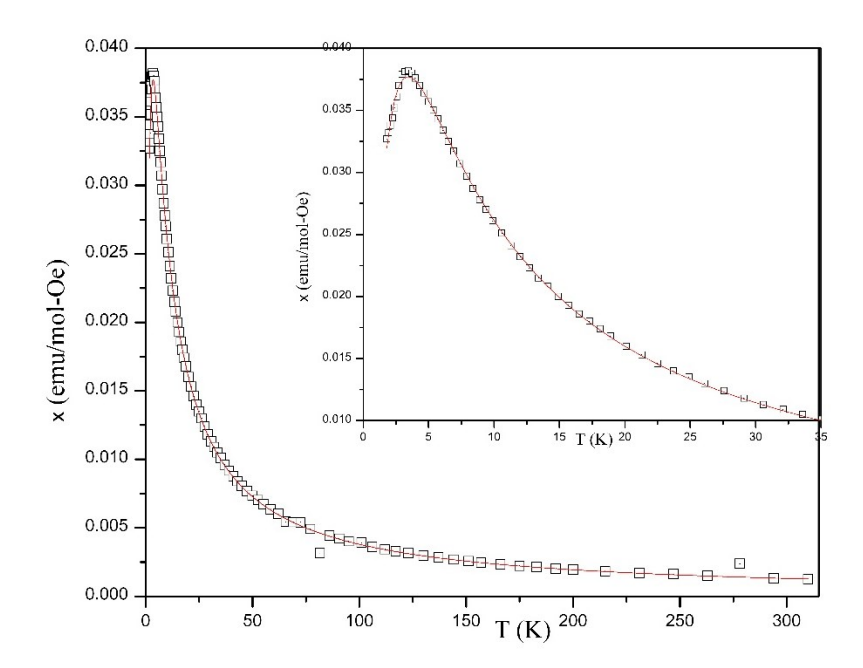


Figure 16. $\chi(T)$ data for 3. The solid lines show the best fit to the uniform chain model with a Curie-Weiss correction for interchain interactions. The inset shows an expansion of the region near the maximum in χ .

DISCUSSION

The structure of the chloride compound 1 is unusual in the regard that although the two 5IAP ligands are in the syn-conformation, dimer formation does not occur as would be expected.³⁵ The lack of magnetic exchange interactions is also surprising, but readily explained by the crystal structure. The presence of a water molecule in the lattice, and the corresponding hydrogen bonds, provides additional separation between the molecules of 1, and the strong halogen bonds observed between the chloride ions and highly polarizable iodine atoms prevent close contact between the chloride ions, thus eliminating the two-halide mechanism as a superexchange pathway.³⁴ On the other hand, the 5IAP ligands in the bromide complex, 2, also adopt a synconformation and do form the expected dimeric structure via a bihalide bridge between the Cu(II) ions. Magnetic data are well described by the dimer model and show the expected singlet ground state for such a system. The large value of the Curie-Weiss correction for interdimer interactions (-5 K, $\sim 20\%$ of J/k_B), however, is surprising given the distance between the dimers, which would suggest better isolation. Closer examination of the structure reveals two possible two-halide superexchange pathways between dimers, one between Br2 ions ($d_{X cdots X} = 5.20 \text{ Å}$, $\angle_{\text{Cu-X}\cdots\text{X'}} = \angle_{\text{X}\cdots\text{X'-Cu'}} = 171^{\circ}$, $\angle_{\text{Cu-X}\cdots\text{X'-Cu'}} = 180^{\circ}$, Symm. Op. = 1-x, 3-y, 3-z) and one between Br1 ions $(d_{X cdots X} = 5.18 \text{ Å}, \angle_{Cu-X cdots X'} = \angle_{X cdots X'-Cu'} = 177^{\circ}, \angle_{Cu-X cdots X'-Cu'} = 180^{\circ}, \text{ Symm. Op.} = 1-x, 2-x$ y, 2-z). Although both are longer than the normal expected cutoff for such interactions (~ 5 Å), it has been shown that Cu-X···X' angles approaching 180° and Cu-X···X'-Cu' torsion angles approaching either 0° or 180° maximize the exchange.³⁴ Both of these pathways show excellent bond angles and torsion angles which may explain the strength of the interaction even over so large a distance. At shorter distances (3.6 Å), superexchange of -234 K has been observed in a copper(II) bromide complex with similar geometry. The magnitude of the Weiss constant compared to J, suggested that an alternating chain magnetic model might be more appropriate, but attempts to fit the data to that model gave significantly poorer results, especially the quality of fit near the maximum.

The control of structural polymorphism by a simple change in solvent, ethanol to methanol, makes preparation of 2 and its polymorph, 3, convenient. Although some contamination is occasionally observed, the difference in the colors and morphology of the crystals makes isolating a single polymorph straightforward. Compound 3, in its anti-conformation, does not form a bihalide bridged dimer, as observed in 2, but rather the classic bihalide bridged chains

that are commonly seen in such square-planar complexes (Figure 7). This provides a common superexchange pathway and modest exchange was observed which was well described by the uniform chain model (J/k_B \sim -6 K). Weak, interchain interactions ($\theta \sim$ -0.7 K) are in good agreement with the crystal structure which shows isolation of the chains (Figure 8b).

Conclusions

A (5IAP)_nCuX₂, (1-4) family of compounds has been synthesized and the structures have been confirmed through single crystal X-ray analysis. Both 1 and 2 crystallize as ML₂X₂ compounds with the 5IAP ligands in the *syn*-conformation, but only 2 forms the dimeric structure expected of that conformation. The presence of a lattice water molecule in 1 may account for the difference. Variable temperature and field magnetic measurements were made on 1-3. 1 shows only paramagnetic behavior, while 2-3 behave as antiferromagnets and were successfully modeled as a dimer and uniform chain, respectively. Development of synthetic methods to produce sufficient quantities of pure 4 for analysis of magnetic properties are in progress.

Acknowledgements:

We gratefully acknowledge financial assistance from the National Science Foundation (NSF) for grants to purchase the SQUID magnetometer (IMR-0314773) and toward the purchase and construction of a helium recycling system (DMR-1905950). DAD is grateful for MRI grant CHE-2018870 from the NSF toward the purchase of the single-crystal diffractometer. Contributions from SEQENS toward the purchase of the powder X-ray diffractometer and from the Kresge Foundation for the purchase of both the SQUID and X-ray diffractometer are also greatly appreciated. NVH is grateful for a Maureen Milburn summer research fellowship.

Supplementary Information:

CCDC contains the supplementary crystallographic data for: **1**, 2277029; **2**, 2277030; **3**, 2277031; **4**, 2277032. These data can be obtained free of charge via http://www.ccdc.cam.ac.uk/conts/retrieving.html, or from the Cambridge Crystallographic Data Centre, 12 Union Road, Cambridge CB2 1EZ, UK; fax: (+44) 1223-336-033; or e-mail: deposit@ccdc.cam.ac.uk.

References

1. Olivier Kahn, *Molecular Magnetism*, VCH Publishers, Inc., New York (1993). Dover Edition, Garden City, NY (2021).

- 2. D.J. Hodgson., Prog. in Inorg. Chem. 19 (1975) 173.
- 3. M.T. Batchelor, X.W. Guan, N. Oelkers, Z. Tsuboi. Adv. Phys., 56 (2007) 465.
- 4. L. Lezama, A. Luque, T. Rojo, P. Roman, J. Sertucha. J. Chem. Soc., Dalton Trans. (1997) 847.
- 5. M. Mitra, P. Manna, A. Das, S.K. Seth, M. Helliwell, A. Bauzá, S.R. Choudhury, A. Frontera, S. Mukhopadhyay. J. Phys. Chem. A. 117 (2013) 5802.
- 6. J. Abdelhak, E. Badjaa, N. Essghaier, R. Hanene, A. Naouar, F.M. Zid, N. Sadfi-Zouaoui. J. Microbiol, Biotech, and Food Sci., 4 (2015) 225.
- 7. S. Banerjee, A. Bieńko, D. Bieńko, D. Bose, K. Das Saha, S. Goswami, R. Modak, Y. Sikdar, W. Zierkiewicz. Dalton Trans., 44 (2015) 8876.
- 8. K. Dunbar. Inorg. Chem., 51 (2012) 12055.
- 9. R.T. Butcher, J.J. Novoa, J. Ribas-Ariño, A.W. Sandvik, M.M. Turnbull, C.P. Landee, B.M. Wells, F.F. Awwadi., Chem. Commun., 11 (2009) 1359.
- 10. W.E. Marsh, W.E. Hatfield, D.J. Hodgson. Inorg. Chem., 21 (1982) 2679.
- 11. W.E. Marsh, D.S. Eggleston, W.E. Hatfield, D.J. Hodgson. Inorg. Chim. Acta., 70 (1983) 137.
- 12. J. Anagnostis, J. Cipi, C.P. Landee, G.W. Tremelling, M.M. Turnbull, B. Twamley, J.L. Wikaira. J. Coord. Chem., 70 (2017) 3892.
- 13. R.A. Ahmani, S. Amani, R. H.A. Khavasi, N. Safari. J. Coord. Chem., 64 (2011) 2056.
- 14. J. Abdelhak, S.N. Cherni, A. Driss, M.F. Zid. J. Struct. Chem., 56 (2015) 654.
- 15. J. Abdelhak, I. Cherif, A. Driss, M.F. Zid. Annales de Chimie., 37 (2012) 61.
- 16. M. Deumal, J. Jornet, L. Li, C.P. Landee, M.M. Turnbull, J.L. Wikaira. Inorg. Chem., 46 (2007) 11254.
- 17. A.S. Albrecht, D.C. Dender, P.R. Hammar, C.P. Landee, D.H. Reich. J. Appl. Phys., 81 (1997) 4615.
- 18. A.S. Albrecht, C.P. Landee, M.M. Turnbull, F.M. Woodward, C.M. Wynn. Phys. Rev. B., 65 (2002) 144412.
- 19. J. Giantsidis, C.P. Landee, M.M. Turnbull, F.M. Woodward. Inorg. Chim. Acta., 324 (2001) 324.

- 20. M.A. Abdalrahman, F.F. Awwadi, G.B. Jameson, C.P. Landee, C.G. Saunders, M.M. Turnbull, J.L. Wikaira. CrystEngComm., 15 (2013) 4309.
- 21. C. Galeriu, J. Giantsidis, C.P. Landee, M.M. Turnbull. J. Coord. Chem., 55 (2002) 795.
- 22. C. Galeriu, J. Giantsidis, C.P. Landee, M.M. Turnbull. Phys. Rev. B., 63 (2001) 100402.
- 23. J.E. Chellali, C.L. Chittim, P.C. Farris, C.P. Landee, M.M. Turnbull, A.D. Wall, J.L. Wikaira. J. Coord. Chem., 71 (2018) 2487.
- 24. Bruker AXS Inc., Madison, WI, USA, (2012).
- 25. L. Krause, R. Herbst-Irmer, G. M. Sheldrick, D. Stalke J. Appl. Cryst. 48 (2015) 3.
- 26. SMART: v.5.626, Bruker Molecular Analysis Research Tool, v.5.626; Bruker AXS: Madison, WI, 2002.
- 27. SAINTPlus: v. 6.36a, Data Reduction and Correction Program, Bruker AXS, Madison, WI, 2001.
- 28. <u>CrystalClear</u>: Rigaku Corporation, 1999. CrystalClear Software User's Guide, Molecular Structure Corporation, (c) 2000. J.W.Pflugrath Acta Cryst. D55 (1999) 1718.
- 29. Higashi, T. (1995) Program for Absorption Correction. Rigaku Corporation, Tokyo.
- 30. G.M. Sheldrick. Acta Crystallogr. A Found. Crystallogr., 64 (2008) 112.
- 31. G.M. Sheldrick. Acta Crystallogr., Sect. C, 71 (2015) 3.
- 32. P.C. Farris, A.D. Wall, J.E. Chellali, C.L. Chittim, C.P. Landee, M.M. Turnbull, J.L. Wikaira J. Coord. Chem. 71 (2018) 2487.
- 33. C.R. Groom, I.J. Bruno, M.P. Lightfoot, S.C. Ward, Acta Cryst.. B72 (2016) 171. CSD Version 5.44, April 2023.
- 34 M.M. Turnbull, C.P. Landee, B.M. Wells, Coord. Chem. Rev. 249 (2005) 2567.
- 35. R.J. DuBois, C.P. Landee, M. Rademeyer, M.M. Turnbull, J. Coord. Chem. 72 (2019) 1785.
- 36. J. Giantsidis, C. Galeriu, C.P. Landee, M.M. Turnbull J. Coord. Chem. 55 (2002) 795.
- 37. D.J. Carnevale, L.N. Dawe, C.P. Landee, M.M. Turnbull, J.L. Wikaira Polyhedron 202 (2021) 115200.
- 38. A.W. Addison, T.N. Rao, J. Reedijk, J. van Rijn, G.C. Verschoor, J. Chem. Soc. Dalton. Trans., (1984) 1349.
- 39. C.L. Chittim, K. Faber, D.A. Dickie, C.P. Landee, S.G. Telfer, M.M. Turnbull, J. Coord. Chem. 76 (2023) in press.
- 40. J. Emsley, M. Arif, P.A. Bates, M.B. Hursthouse Inorg. Chim. Acta 143 (1988) 25.
- 41. W. Henke, S. Kremer, D. Reinen Inorg. Chem. 22 (1983) 2858.

- 42. M.I. Arriortua, J.L. Mesa, T. Rojo, T. Debaerdemaeker, D. Beltran-Porter, H. Stratemeier, D. Reinen Inorg. Chem. 27 (1988) 2976.
- 43. A. Kutoglu, R. Allmann, J.-V. Folgado, M. Atanasov, D. Reinen Z. Naturforsch B:Chem.Sci. 46 (1991) 1193.
- 44. R.L. Forman, A.J. Gale, C.P. Landee, M.M. Turnbull, J.L. Wikaira Polyhedron 89 (2015) 76.
- 45. C.P. Landee, M.M. Turnbull J. Coord. Chem. 67 (2014) 375.